Improving Image Segmentation Performance via Edge Preserving Regularization

Ying-jie Zhang   Li-ling Ge

Abstract—This paper presents an improved image segmentation model with edge preserving regularization based on the piecewise-smooth Mumford-Shah functional. A level set formulation is considered for the Mumford-Shah functional minimization in segmentation, and the corresponding partial difference equations are solved by the backward Euler discretization. Aiming at encouraging edge preserving regularization, a new edge indicator function is introduced at level set frame. In which all the grid points which is used to locate the level set curve are considered to avoid blurring the edges and a nonlinear smooth constraint function as regularization term is applied to smooth the image in the isophote direction instead of the gradient direction. In implementation, some strategies such as a new scheme for extension of u^+ and u^- computation of the grid points and speedup the convergence are studied to improve the efficacy of the algorithm. The resulting algorithm has been implemented and compared with the previous methods, and has been proved efficiently by several cases.

Keywords—Energy minimization, image segmentation, level sets, edge regularization.

I. INTRODUCTION

THE segmentation of structure from 2D and 3D images is one of the most important steps in analyzing image data. For example, in medical fields, it is necessary to segment the brain in an MR image, before it can be rendered in 3D for visualization purposes. The main goal of segmentation is to identify an image as a collection of features, each of which has a strong correction with real-world objects. Another important application is registration. It may be easier or at least less error prone to segment objects in multiple images prior to registration. This is especially true in images from different modalities.

Mumford-Shah functional is a widely used variational model for image analysis [1]. It minimizes an energy functional involving a piecewise smooth representation of an image by viewing an active contour as the set of discontinuities, resulting in simultaneous linear restoration and segmentation [2]. However, on one hand, a potential problem with this approach is that the topology of the region to be segmented must be known in advance. An algorithm to overcome these difficulties was first introduced by Osher and Sethian [3]. They model the propagating curve as a specific level set of a higher dimensional surface. It is common practice to model this surface as a function of time. So as time progresses, the surface can change to take on the desired shape. On the other hand, the Mumford-Shah functional is based on Bayesian linear restoration, so the resultant homogenous smoothing may blur true boundaries [15]. The situation becomes worse for poor quality images like medical images with low contrast and artifacts, making the coupled segmentation unreliable. Researchers have done a lot of works [4, 5] on Mumford-Shah functional to obtain edge-preserving regularization. In [4], an edge function varying from zero to one is defined over the entire image and an elliptic approximation for arc lengths is introduced. The functional can perform edge-preserving diffusion controlled by the edge function, but it cannot develop shocks. Aiming at this point, Jayant Shah [5] proposed a new segmentation functional where the smooth constraint and the data fidelity are defined by the norm functions instead of quadratic functions. It can develop singular points and deblur the edge. However, these models use the elliptic approximation and Γ-convergence. It results in solving a family of the coupled partial differential equations: one for the intensity image, the other for edge, which may bring expensive computational cost. Moreover, the obtained boundary is not continuous by introducing the edge function. In [6], an edge-preserving regularization model based on the half-quadratic theorem is proposed that can perform both edge-preserving restoration and edge detection. Although the elliptic approximation is not used in this model, it is similar to the previous work [4, 5] and the numerical implementation still involves in solving a set of the coupled partial differential equations.

Regularization algorithms have attracted a growing interest in computer vision community. It consists in simplifying data in a way that only interesting features are preserved. On basis of the key idea of the diffusion theory, the improved Mumford-Shah functional is introduced by using a piecewise non-linear function as regularization terms instead of the smooth constraint term. Roughly speaking, the regularization term may be seen as non-linear filters that simplify the image little by

Ying-jie Zhang is with school of mechanical engineering, Xi'an Jiaotong University, Xi'an, Shaanxi, People's Republic of China. His research interests are image segmentation and 3-Dvisualization (email: yjzhang@mail.xjtu.edu.cn).

Li-ling Ge is with School of Material Engineering, Xi'an University of Technology, Xi'an, Shaanxi, People's Republic of China. Her research interests are metallographic analysis and image segmentation (email: Geliling-xut@163.com).

World Academy of Science, Engineering and Technology
International Journal of Computer and Information Engineering
Vol:2, No:3, 2008

little and minimize then image variations. Note therefore that it allows the coupled edge-preserving diffusion and image segmentation. Different from the previous work as follows. First, the non-linear constraint function is applied as regularization term to make images close to the ideal restoration, thus facilitating the boundary finding. Second, all the grid points that is used to locate the evolving front are considered in the smoothing process. Thus, the better edge-preserving properties may be obtained. Finally, in implementation, some strategies such as the improved scheme for extension of the function u^+ and u^-, computation of the discrete points and speedup of the convergence are also studied The rest of this paper is organized as follows. Section 2 introduces the level set theory and Mumford-Shah functional. Section 3 describes the proposed approach, and Section 4 studies some new strategies such as an improved scheme for the extension of u^+ as well as u^-, computation of the grid points and speedup of the convergence. Some results of numeric experiments are given in Section 5, which is followed by conclusion in Section 6.

II. LEVEL SET AND MUMFORD-SHAH MODEL

In this section, let's briefly review the level set model and Mumford-Shah functional in image process.

A. Level Set Model

Let Ω be a bounded open subset of R^2, with Γ as its boundary. Then a two dimensional image u_0 can be defined as $u_0 : \Omega \to R$. In this case Ω is just a fixed rectangular grid. Now consider the evolving curve Γ in Ω, as the boundary of an open subset ω of Ω. In other words, $\omega \in \Omega$, and Γ is the boundary of ω. This idea is to embed this propagating curve as the zero level set of a higher dimensional function ϕ, which is defined as follows:

$$\phi(x, y, t = 0) = \pm d \qquad (1)$$

where d is the distance from (x, y) to $\partial\omega$ at t = 0, and the plus or minus sign is chosen if the point (x, y) is outside or inside the subset ω. Now, the goal is to make an equation for the evolution of the curve. Evolving the curve in the direction of its normal amounts to solving the partial differential equation [3]:

$$\frac{\partial \phi}{\partial t} = F \left| \nabla \phi \right|$$

$$\phi(x, y, 0) = \phi_0(x, y) \qquad (2)$$

where the set $\{(x, y), \phi_0(x, y) = 0\}$ defines the initial contour, and F is the speed of propagation.

For certain forms of the speed function F, this reduces to a standard Hamilton-Jacobi equation. There are several major advantages to this formulation. The first is that $\phi(x, y, t)$ always remains a function as long as F is smooth. As the surface ϕ evolves, the curve Γ may break, merge, and change topology.

B. Mumford-Shah Model

Let u_0 be the given image, under the assumption that the desired contours (denoted by Γ) in the image can be represented by level set functions. The Mumford-Shah functional is defined as the minimization of the functional [1]:

$$E_{MS}(u, \Gamma) = \upsilon Length(\Gamma) + \lambda \int_\Omega |u - u_0|^2 dx + \mu \int_{\Omega \backslash \Gamma} |\nabla u|^2 dx \qquad (3)$$

where υ, λ and μ are non-negative constants, and u is a cartoon image that is locally smooth, except for near Γ. Image segmentation can be carried out by minimizing $E_{MS}(u, \Gamma)$ over an appropriate space. In fact, Γ denotes the set of discontinuity points of u and the length of Γ denotes the cardinal of Γ.

As discussed earlier in the level set models, let $\{(x, y), \phi(x, y) = 0\}$ define the contour Γ and two functions u^+ and u^- are introduced, such that [8]:

$$u(x) = u^+ H(\phi(x)) + u^- (1 - H(\phi(x))) \qquad (4)$$

where H(x) is the Heaviside function, $\delta(z)$ as its derivativeness.

These two functions replace the two unknown constants used in [8]. For the piecewise-smooth Mumford-Shah functional, this two functions u^+ and u^- are assumed that are C^1 functions on $\phi \geq 0$ and $\phi < 0$, respectively, and with continuous derivatives up to all boundary points, i.e. up to the boundary $\{\phi = 0\}$. Therefore, the following minimization problem is obtained from the piecewise-constant Mumford-Shah functional [1]:

$$\inf_{u^+, u^-, \phi_0} E_{MS}(u^+, u^-, \phi) = \lambda \int_\Omega |u^+ - u_0|^2 H(\phi) dx$$
$$+ \lambda \int_\Omega |u^- - u_0|^2 (1 - H(\phi)) dx + \mu \int_\Omega |\nabla u^+|^2 H(\phi) dx$$
$$+ \mu \int_\Omega |\nabla u^-|^2 (1 - H(\phi)) dx + \upsilon \int_\Omega |\nabla H(\phi)| \qquad (5)$$

Then with ϕ fixed, the equation (3) leads to the two Euler-Lagrange equations for u^+ and u^- written as

$$\begin{cases} u^+ - u_0 = \mu \Delta u^+ & \{(x) : \phi(x, t) > 0\} \\ \dfrac{\partial u^+}{\partial \vec{n}} = 0 & \{(x) : \phi(x, t) = 0\} \cup \partial\Omega \\ u^- - u_0 = \mu \Delta u^- & \{(x) : \phi(x, t) < 0\} \\ \dfrac{\partial u^-}{\partial \vec{n}} = 0 & \{(x) : \phi(x, t) = 0\} \cup \partial\Omega \end{cases} \qquad (6)$$

Notice that u^+ and u^- act as denoising process on the homogeneous regions only. No smoothing is done across the boundary $\{\phi = 0\}$, which is very important in image analysis.

Now, keeping u^+ and u^- fixed, and minimizing $E_{MS}(u^+, u^-, \phi)$ with respect to the function ϕ, one can

World Academy of Science, Engineering and Technology
International Journal of Computer and Information Engineering
Vol:2, No:3, 2008

obtain the motion of the zero level set as following:

$$\frac{\partial \phi}{\partial t} = \delta(\phi)(\upsilon \nabla (\frac{\nabla \phi}{|\nabla \phi|}) - \lambda |u^+ - u_0|^2 - \mu |\nabla u^+|^2 \qquad (7)$$

$$+ \lambda |u^- - u_0|^2 + \mu |\nabla u^-|^2)$$

The above equation (7) with some initial guesses ϕ (t=0, x) is actually computed at least near a narrow band of the zero level set. As a result, computationally, one has to continuously extend both u^+ and u^- from their original domain $\{\pm \phi > 0\}$ to a suitable neighborhood of the zero level set $\{\phi = 0\}$. Although u^+ and u^- can be easily obtained by solving Euler-Lagrange equations (6), the extensions of u^+ and u^- are difficult to be obtained as solution of the following degenerate elliptic linear equations:

$$\begin{cases} u_t^+ = \nabla^2 u^+ (\vec{N}, \vec{N}) & \{\phi < 0\} \\ \frac{\partial u^+}{\partial \vec{n}} = 0 \end{cases} \qquad (8)$$

and

$$\begin{cases} u_t^- = \nabla^2 u^- (\vec{N}, \vec{N}) & \{\phi > 0\} \\ \frac{\partial u^-}{\partial \vec{n}} = 0 \end{cases} \qquad (9)$$

Chan and Vese [9] had pointed out three possible ways to solve the problem, but all of them were difficult to carry out practically.

III. IMPROVED MODEL

Consider that under level set frame, the evolving front is obtained from some grid points in image spaces. In previous works [4, 5], the edges are supposed as a precise curve, the corresponding edge indicator function [6,13] is determined based on points of the ideal curves. However, the edges which are traced by level set curve at level set frame are given by some grid points with signed distance close to zero. It is impossible to find theoretically the precise boundary at discrete image space. Therefore, some approximate approaches should be searched to close to the ideal curves.
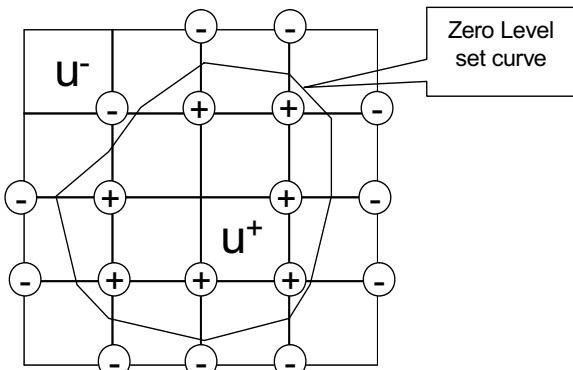

Fig. 1 The level set front and the corresponding grid points at image space

Aiming at this point, as shown in Fig. 1, let χ denotes the set of the grid points. A new edge indicator function is defined as follows:

$$\xi(x) = \begin{cases} \eta(x), & x \in \chi \\ 1, & otherwise \end{cases} \qquad (10)$$

where $\eta(x)$ is a non-negative function with values from 0 to 1. If a point is on the ideal curve then $\eta(x) = 0$, otherwise $\eta(x)$ is applied to calculate how much the point's contribution for the ideal curves. Let $\phi(x)$ denote the signed distance function of the current point, $\|\phi_2(x) - \phi_1(x)\|$ denote the distance of the nearest two points to the ideal curve, then $\eta(x)$ can be obtained by:

$$\eta(x) = \frac{|\phi(x)|}{\|\phi_2(x) - \phi_1(x)\|} \qquad (11)$$

Furthermore, the smooth constraint term $|\nabla u|^2$ in (3) is replaced by a nonlinear function $\Psi(|\nabla u|)$. There are a lot of $\Psi(x)$ functions listed in [8], together with some of their properties. The improved Mumford-Shah function is given by:

$$E_{MS}(u, \Gamma) = \upsilon Length(\Gamma) + \lambda \int_\Omega |u - u_0|^2 dx$$

$$+ \mu \int_{\Omega \backslash \Gamma} \xi(x) \cdot \Psi(|\nabla u|) dx \qquad (12)$$

where $\Psi(x)$ is a nonlinear function as regularization energy term. To encourage edge-preserving regularization, $\Psi(x)$ should be close to constant in the interior of the region and close to zero on boundaries. The Euler-Lagrange equation corresponding to this minimization problem is given by:

$$\frac{1}{2} \cdot \frac{dE}{du} = \lambda(u - u_0) - \mu \cdot div(\xi \cdot \frac{\Psi'(\|\nabla u\|)}{\|\nabla u\|} \nabla u) = 0 \qquad (13)$$

This equation corresponds to the steady state of the following diffusion process:

$$\frac{\partial u}{\partial t} = \mu \cdot div(\xi \cdot \frac{\Psi'(\|\nabla u\|)}{\|\nabla u\|} \nabla u) + \lambda(u_0 - u) \qquad (14)$$

Then as known in section 2, let $u(x) = u^+ H(\phi(x)) + u^-(1 - H(\phi(x)))$, embedding the evolving front as the zero level set of a higher dimensional function ϕ and normal of the curve is given as $\vec{N} = -\frac{\nabla \phi}{|\nabla \phi|}$, the corresponding level set evolution equation is given as follows:

$$\frac{\partial \phi}{\partial t} = \delta(\phi)\{\mu \cdot \xi(\phi)(\Psi(|\nabla u^-|) - \Psi(|\nabla u^+|))$$

$$+ \lambda(|u^- - u_0|^2 - |u^+ - u_0|^2) + \upsilon \cdot \nabla(\frac{\nabla \phi}{|\nabla \phi|})\} \qquad (15)$$

where u^- and u^+ represent the points in the interior and exterior of the current curve respectively.

World Academy of Science, Engineering and Technology
International Journal of Computer and Information Engineering
Vol:2, No:3, 2008

IV. Some Strategies in Implementation

A. Strategy for the extension of functions u^+ and u^-

Known from the previous sections, Chan and Vese in [8] proposed an approximate approach for extensions of u^+ and u^- as following:

$$u_{i,j}^{\pm,n+1} = (u_{i-1,j}^{\pm,n} + u_{i+1,j}^{\pm,n} + u_{i,j-1}^{\pm,n} + u_{i,j+1}^{\pm,n})/4 \qquad (16)$$

Note that the differences between the images u_0 and u^+ or u^- in (7) are an important component for evolution of the level set function ϕ. Equation (16) shows two major drawbacks. One is that the current point doesn't be taken into account and some important information such as boundary points may be skipped in the diffusion process. As a result, the true boundaries may be blurred, even disappear in finite number of iterations. Another is that although the noises can be removed efficiently by this method, however, the evolving curves can sway around the true boundaries because of lost of true boundary information. For attack these problems, in our scheme, a new approach to extensions of both u^+ and u^- are introduced. The modified extending function is given by:

$$u_{i,j}^{\pm,n+1} = \frac{1}{4}u_0(i,j) + \frac{1}{8}(u_{i-1,j}^{\pm,n} + u_{i+1,j}^{\pm,n} + u_{i,j-1}^{\pm,n} + u_{i,j+1}^{\pm,n})$$
$$+ \frac{1}{16}(u_{i-1,j-1}^{\pm,n} + u_{i-1,j+1}^{\pm,n} + u_{i+1,j-1}^{\pm,n} + u_{i+1,j+1}^{\pm,n}) \qquad (17)$$

The modified extending function considers the current point and its 8-neighbour points. As a result, more information is remained. Combining with the edge preserving function, even at weak boundaries, this approach can provide proper speed to propagate the front.

B. Strategy to determine the involved points of the boundary curves

It should be noted that under level set frame, the level set functions is obtained by using signed distance function at some discrete points. To encourage edge preserving regularization, all of these discrete points should be avoided blurring in smoothing process to avoid blurring true edges. In our implementation, a temporary buffer which has the same size with the segmented image size is defined to store as the signed distance function and in which the corresponding positions of the discrete points are set as zero so that it can be used to locate and process the discrete points for the smoothing process. Therefore only points with non-zero values in the temporary are allowed to carry out smoothing or diffusion process.

C. Strategy for speedup of the convergence

As the piecewise Mumford-Shah approach, for general noisy images, since its global minimization properties of the energy function speed of the convergence may become more and more slowly with evolution of the curves and the image diffusion. Especially, when the evolving curve is close to convergence, most of the time (tens or even hundreds times), has to be spent up to steady state. For example, as shown in Fig 2, here, n is the number of iterations. For attacking this problem, consider that diffusions of u^+ and u^- are performed on interior of and exterior of the regions, respectively. Therefore difference of energy at both sides of the boundaries would be increased if different number of iterations are applied to calculate the extension of u^+ and u^-. Consequently, the convergence can be speeded up and it has been demonstrated by experiment. As determination of the number of iterations in the classical Mumford-Shah approach, however, how to determine the different numbers of iterations for extension of u^+ and u^- still needs to be researched further. In contrast, for the same image, the segmentation process shown in Fig. 2 with the same iteration 50 for the extensions of both u^+ and u^- is slower than that shown in Fig. 3 with different iterations for extensions of u^+ and u^- as 50 and 10, respectively.
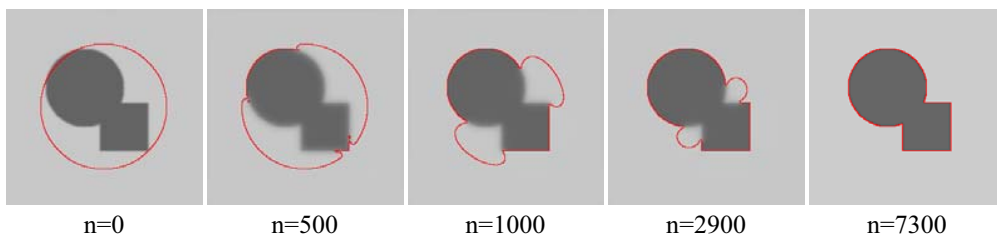

| n=0 | n=500 | n=1000 | n=2900 | n=7300 |

Fig 2 Segmentation process with the same the number of iterations for extensions of u^+ and u^-

| n=0 | n=300 | n=800 | n=1200 | n=1500 |
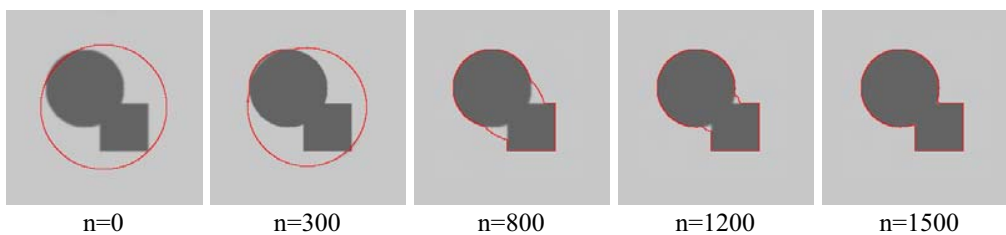
Fig 3 Segmentation process with the different iterations for extensions of u^+ and u^-

World Academy of Science, Engineering and Technology
International Journal of Computer and Information Engineering
Vol:2, No:3, 2008

V. NUMERIC EXPERIMENTS

To demonstrate the validity of the proposed approach, several images are also applied to test it. One of examples is a CT pulmonary vessel image where the vessels and their branches, which exhibit much variability with low contrast and artifacts, make the segmentation difficult. Here $\Psi(x) = \beta \cdot (\sqrt{1+x^2} - 1)$ with β as positive constant is selected in order to encourage smoothing within a region and preserving the boundaries and the other parameters are the same with Chan-Vese approach in [8] as comparison. As shown in Fig. 4, for the same an image, the result by the proposed approach with nonlinear diffusion and coupled edge-preserving regularization is shown in (a) and the result by the piecewise smooth Mumford-Shah approach (coupled homogenous linear diffusion) is shown in (b). It can be seen that the proposed approach performs edge-preserving

regularization better. The vessels even their thin branches could be extracted precisely by using smoothing the interior of the vessel branches and holding the boundary deblurred. In contrast, the important edge site is blurred in the classical approach; therefore, the boundaries become obscure, thereby misleading the curve deforming. As a result, thin vessel branches could not be extracted precisely.

Figure 5 compares the classical method with the proposed algorithm on an image which some object with weak edge. The results show that the proposed algorithm, combined with different number of iterations for extension of u^+ and u^-, can find the object with weak edges, as shown in Fig. 5a and the result by the piecewise smooth Mumford-Shah approach is shown in (b), it can be noticed that the weak object has been disappeared from the resulting segmentation.
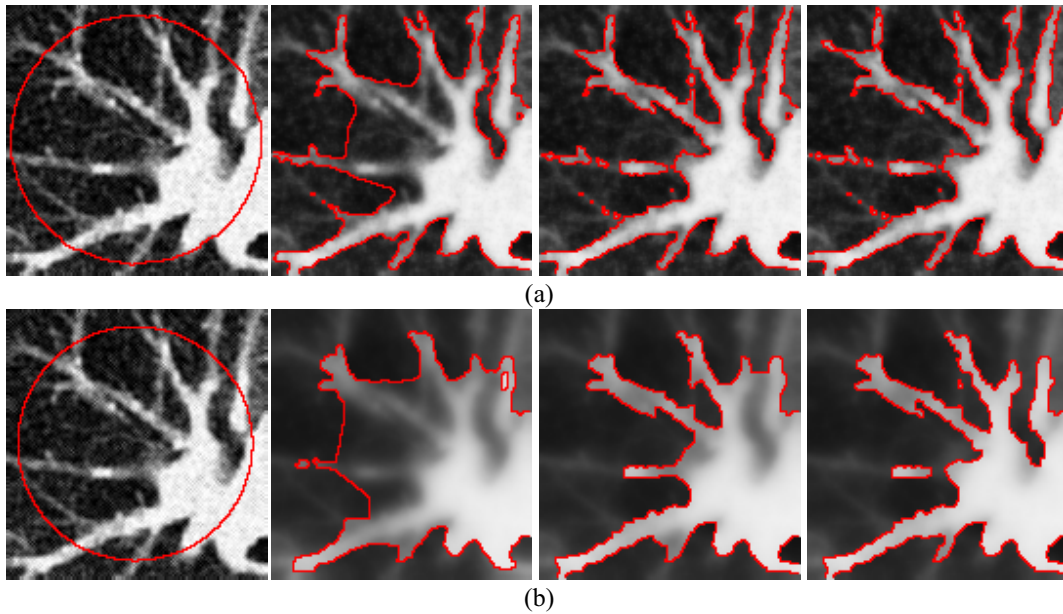

(a)

(b)

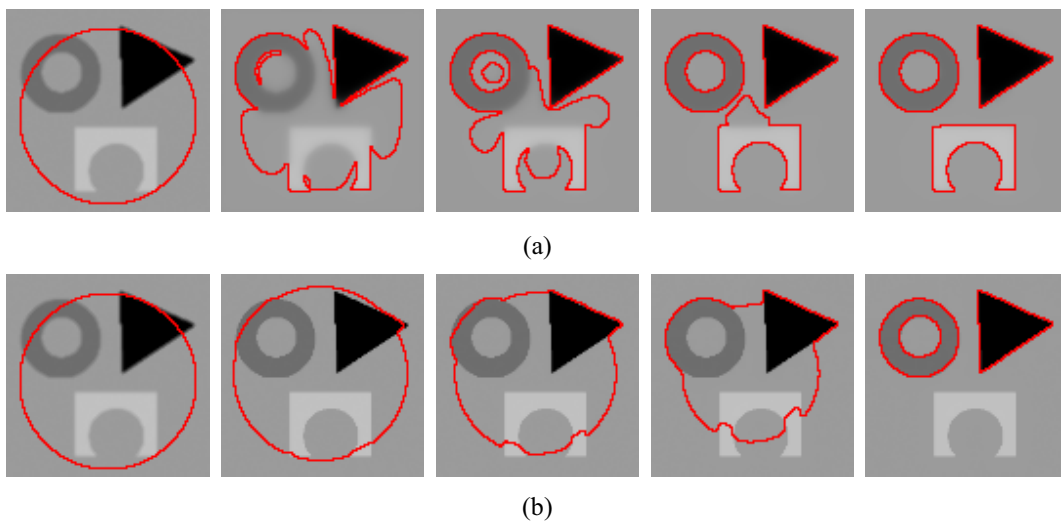Fig. 4 Coupled diffusion and curve evolution (a) by the improved algorithm (b) by classical approach

(a)

(b)

Fig. 5 Coupled diffusion and curve evolution for an image with weak objects (a) by the improved algorithm (b) by classical approach

World Academy of Science, Engineering and Technology
International Journal of Computer and Information Engineering
Vol:2, No:3, 2008

VI. CONCLUSION

In this paper, an image segmentation model for image segmentation with edge preserving regularization is proposed. By introducing a new edge indicator function and nonlinear smoothing function at the piecewise smooth Mumford-Shah functional. And some strategies are purposed to improve the smoothing process and accelerate the evolution of curves. However, as the previous works [8], there are still some difficulties to be solved, such as the segmented results depending on the initial signed distance function, speed of the evolving curve connecting closely choice of the parameters, and so on, they will be research further in our future work.

REFERENCES

[1] D. Mumford and J. Shah, "Optimal approximations by piecewise smooth functions and associated variational problems," *Commun. Pure Appl. Math.*, vol. 42, pp. 577-685, May. 1989.

[2] M. Kass, A. Witkin, and D. Terzopoulos, "Snakes: Active contour models," International Journal of Computer Vision, vol. 1, no. 4, pp. 321–331, 1988.

[3] P. Perona and J. Malik, "Scale space and edge detection using anisotropic diffusion," IEEE Transactions on Pattern Analysis and Machine Intelligence, vol. 12, no. 8,pp. 629–639, 1990.

[4] L. Ambrosis, and V. M. Tortorelli, *On the approximation of functionals depending on Jumps by quadratic elliptic functionals.* Bull. Un. Mat. Ital. 1992

[5] Jayant Shah, "A common framework for curve evolution, segmentation and anisotropic diffusion," in IEEE *Proc. Conf. Computer Vision and Pattern Recognition*, San Francisco, CA, Jun. 1996, pp. 136-142.

[6] S. Teboul, L. B. Féraud, G. Aubert, and M. Barlaud, "Variational approach for edge-preserving regularization using coupled PDE's," *IEEE Trans. Image Processing*, vol.7, no.3, pp.387-397, Mar. 1998.

[7] J. A. Sethian, *Level Set Methods and Fast Marching Methods: Evolving interfaces in computational geometry, fluid mechanics, computer vision and material science.* Cambridge Univ. Press, 1999.

[8] T. F. Chan and L. A. Vese, "A Level Set Algorithm for Minimizing the Mumford-Shah Functional in Image Processing," IEEE Comput. Soc. Proc. of the First IEEE Workshop on Variational and Level Set Methods in Computer Vision, pp. 161–168, 2001.

[9] T. F. Chan and L. A. Vese, "Active Contours without edges," IEEE Transactions on Image Processing, vol. 10, no. 2, pp. 266-277, 2001.

[10] L. A. Vese and T. F. Chan, "A multiphase level set framework for image segmentation using the Mumford and Shah model," International Journal of Computer Vision, vol. 50, no. 3, pp. 271-293, 2002.

[11] J. Weickert, K. J. Zuiderveld, B. M. ter Haar Romeny, W. J. Niessen, "Parallel implementations of AOS schemes: A fast way of nonlinear diffusion filtering," in *Proc. IEEE Conf. Image Processing*, Mar.1997, pp.396-399.

[12] A. Tsai, A. J. Yezzi, and A. S. Willsky, "Curve evolution implementation of the Mumford–Sshah functional for image segmentation, denoising, interpolation, and magnification," *IEEE Trans. Image Processing*, vol.10, pp. 1169-1186, Aug. 2001.

[13] S. Osher and J. A. Sethian, "Fronts propagating with curvature dependent speed: Algorithms based on hamilton-jacobi formulation," Journal of Computational Physics, vol. 79, pp. 12–49, 1988.

[14] S. Osher and R. Fedkiw, Level set methods and dynamic implicit surfaces, New York, Springer-Verlag, 2003.

[15] S. Geman, and D. Geman, "Stochastic relaxation, Gibbs distribution and the Bayesian restoration of images," *IEEE Trans. Pattern Anal. Machine Intell.*, vol. PAMI-6, pp.721-741, Nov. 1984.

[16] S. Geman and D. E. Mcclure, "Bayesian image analysis: An application to single photon emission tomography," Proc. Stat. Comput. Sect. Washington, DC: Amer. Stat. Assoc. pp. 12-18, 1985.

[17] S. Ji and H. Park, "Image segmentation of color image based on region coherency," in Proceedings 1998 International Conference on Image Processing, vol. 1, Chicago, IL, USA, pp. 80-83,1998.

[18] S. Kichenassamy, A. Kumar, P. Oliver, A. Tannenbaum, and A. Yezzi, "Conformal curvature flows: from phase transitions to active vision," Archive for Rational Mech. and Anal., vol. 134, pp. 275–301, 1996.

[19] C. Xu and J. Prince, "Snakes, shapes, and gradient vector flow," IEEE Transactions on Image Processing, vol. 7, pp. 359–369, March 1998.

[20] Choi, G. Kim, P. Park, G. Wang, and S. Kim, "Efficient PDE-based segmentation algorithms and their application to CT images," Journal. Korean Institute of Plant Engineering, pp. 1-17, 2003.

[21] J. Haddon and J. Boyce, "Image segmentation by unifying region and boundary information," IEEE Transactions on Pattern Analysis and Machine Intelligence, vol. 12, no. 10, pp. 929–948, 1990.

[22] K. Haris, S. Efstratiadis, N. Maglaveras, and A.Katsaggelos, "Hybeid image segmentation using watersheds and fast region merging," IEEE Transactions on Image Processing, vol. 7, no. 12, pp. 1684–1699, 1998.

[23] D. Marr and E. Hildreth, "Theory of edge detection," Proc. R. Soc. Lond., vol. B207, pp. 187–217, 1980.

[24] P. Hill, C. Canagarajah, and D. Bull, "Texture gradient based watershed segmentation," IEEE International Conference on Acoustics, Speech, and Signal Processing, vol. 4, Orlando, FL, USA, pp. 3381-3384,2002.